T.C.

ALTINBAS UNIVERSITY

Institute of Graduate Studies

Electrical and Computer Engineering

MAGNETIC RESONANCE IMAGING (MRI) FOR BRAIN TUMOR AND SEIZURES CLASSIFICATION USING RECURRENT NEURAL NETWORK

Marwah Riyadh AL-JALEELI

Master of Science

Supervisor

Prof. Dr. Oğuz BAYAT

Istanbul, 2021

MAGNITIC RESONANCE IMAGING (MRI) FOR BRAIN TUMOR AND SEIZURES CLASSIFICATION USING RECURRENT NEURAL NETWORK

By

Marwah Riyadh AL-JALEELI

Electrical and Computer Engineering

Submitted to the Institute of Graduate Studies

in partial fulfillment of the requirements for the degree of

Master of Science

ALTINBAŞ UNIVERSITY

2021

The thesis titled "MAGNETIC RESONANCE IMAGING (MRI) FOR BRAIN TUMOR AND SEIZURES CLASSIFICATION USING RECURRENT NEURAL NETWORK" prepared and presented by "Marwah Riyadh AL-JALEELI" was accepted as a Master of Science Thesis in Electrical and Computer Engineering.

____

Prof. Dr. Oğuz BAYAT

Supervisor

Thesis Defense Jury Members:

Prof. Dr. Oğuz BAYAT	School of Engineering and Natural Sciences, Altinbas University	__________________
Asst. Prof. Dr. Abdullahi Abdu Ibrahim	School of Engineering and Natural Sciences, Altinbas University	__________________
Asst. Prof. Dr. Izzet Parug DURU	Vocational School, Istanbul Gedik University	__________________

I certify that this thesis satisfies all the requirements as a thesis for the degree of Master of Science.

Approval Date of Institute of Graduate Studies: ____/____/____

I hereby declare that all information in this document has been obtained and presented in accordance with academic rules and ethical conduct. I also declare that, as required by these rules and conduct, I have fully cited and referenced all material and results that are not original to this work.

Marwah Riyadh AL-JALEELI

DEDICATION

I dedicate and pledge this thesis work to my supervisor who is salient for guiding me throughout the entire thesis work and my family for continuously support me in my difficult time.

ACKNOWLEDGEMENTS

To begin, I would like to express my gratitude to my supervisor, Prof. Dr. Oğuz BAYAT, for guiding and assisting me in the process of writing this thesis. Debating my progress, challenges, and principles with my supervisor Prof. Dr. Oğuz BAYAT aided me tremendously in comprehending the reasoning behind this study. It improved my understanding of the technical requirements for the research project. Without his time and assistance, this research would not have been possible, and I am grateful to him for providing me with the opportunity to work on such an interesting topic. Additionally, I am indebted to my parents and friends for their unwavering support during this journey.

ABSTRACT

MAGNETIC RESONANCE IMAGING (MRI) FOR BRAIN TUMOR AND SEIZURES CLASSIFICATION USING RECURRENT NEURAL NETWORK

AL-JALEELI, Marwah Riyadh,

M.Sc., Electrical and Computer Engineering, Altınbaş University

Supervisor: Prof. Dr. Oğuz BAYAT

Date: 04/2021

Pages: 52

This research work aims to utilize the developed and evaluated Magnetic Resonance Imaging (MRI) technique for the classification of brain tumor and seizures employing Recurrent Neural Network (RNN). The medical science in the image processing is an emergent area that has suggested many progressive methods in detecting as well as analyzing a specific disease. Brain tumors treatment is recently getting progressively more challenging owing to the intricate shape, structure and the texture of tumor. So, via progressing in the image processing, different methodologies have been suggested for identifying the tumors inside brain. The progression in such area made a need for searching more upon the methods and approaches evolved for the extraction of tumor. Therefore, an extraction system the tumor from the brain is suggested utilizing MRI images. Such method includes various procedures of image processing, like filtering, the removal of noise, segmentation, and morphological processes. Brain tumor extraction can be successfully achieved via conducting such processes upon MATLAB software. The cross-correlation is calculated between the changeable vector of a target and the zone of tumor for determining in what way the values of pixels of the zone of tumor are narrowly associated utilizing the image processing and the RNN method accomplishing 99.71% accuracy. The model being fit to the data till no additional remarkable reduction in the loss function value was performed upon the data of confirmation. It was trained and confirmed till (100) epochs upon precise (200) samples and (65) samples correspondingly with 10-cross fold validation. The measured classification accuracy of the brain tumor at the last epoch of the classifier training of validation data is virtuous.

Keywords: Brain, RNN, Classification, Segmentation, Seizure, Deep learning, MRI

TABLE OF CONTENTS

Pages

LIST OF TABLES

Pages

LIST OF FIGURES

Pages

LIST OF ABBREVIATIONS

AUC	:	Area under consideration
CAD	:	Computer aided diagnosis
CNN	:	Convolutional neural network
DL	:	Deep learning
ROI	:	Region of interest
GPU	:	Graphic processing unit
MRI	:	Magnetic resonance imaging
RNN	:	Recurrent neural network
FCN	:	Fully convolutional network
ML	:	Machine learning

1. INTRODUCTION

The current study proposes an RNN-based technique for segmenting a tumor and removal from an MRI concept and obtaining a connection for the entire disease. To accomplish this, quite a few separation techniques were used; additionally, an overview of the efficacy of the segmentation method was given. Every MRI picture was passed via an imaging sequence, where it was well before to remove noise and enhanced for contrast. Also, this research suggests (5) various segmentation methods which being later implemented upon the image for extracting the tumor. Such methods comprise image segmentation of image, the pre-processing of image, the extraction of feature, the segmentation of watershed, and the conversion of RGB. Implementing each of these segmentation methods permits obtain the highly suitable technique for segmenting the tumor from every image. A normalized cross correlation upon every segmented tumor was later implemented for determining the accuracy. Additionally, the front (tumor) and back (skull) zones of the texture image were used to calculate the cross link between the target variable in addition to the tumor section, to determine how the tumor zone pixels are narrowly correlated with one another. The goal line changeable is a vector that contains two classes:

(0) for the skull zone

(1) for the tumor zone.

The tumor zone means the pixel standards for the front points that were extracted from a surface view using the MATLAB command. The texture image was produced using the RNN technique. To improve the features of the texture of the image, a smoothing filter was implemented to the texture image, and this aids to realize the characteristics of texture more obviously.

The exact solution was firstly solved by applying a new technology. Secondly, in regards of the label imbalance issue in the medical imaging, the object detection techniques were integrated into the semantic segmentation framework of the present study for the purpose of locating ROIs and performing local segmentations. The lesion of localization step imposes an additional level of supervision on training the segmentation networks. The results of the brain tumor segmentation task evinced that the proposed formulated automated RNN can effectively enhance the segmentation accuracy. The results of the brain tumor segmentation task strengthen this enhancement and elucidate that the overall performance produced by combining the formulated RNN post-processing and the lesion localization is better than the conventional methods.

1.1 PROBLEM STATEMENT

The main challenge met was the locating and removing the suitable tumor zone from the image. Owing to some illuminating topics, unessential white portions exist in the image which may possibly incorrectly be segmented such as a tumor. And, the undesirable noise and the decreased contrast view some areas from the image that being incorrectly demanded as a tumor. Additional challenge met was the (MRI) image degraded quality owing to some difficulties that would have taken place through the stage of gaining. As well, removing the characteristics of texture from the image utilizing the proper filters of texture and computing the coefficient of correlation was additional main challenge met. The exposure difficulties have been highly reduced via implementing the proper noise filtering methods such as median filter. Such noise removal procedure eliminates the majority of the undesirable white and black zones from the image. Implementing the proper segmentation methods pursued via various morphological processes assists in retentive merely the pertinent portions of tumor and overpowers the portions of skull of the image to a big range. That will aid in the analysis of the significant portions of the image too capably.

1.2 OVERVIEW

Deep learning is characterized for its automatic feature extraction, thus it combines the feature engineering and the traditional machine learning, as mentioned in [1]. Upon their success in image classification tasks, RNNs were soon applied to the field of semantic segmentation, replacing the old mode of designing hand engineered features in conjunction with decision forests. The recurrent neural network (RNN) was the first end on deep learning model that can perform dense prediction, and its segmentation accuracy was revolutionary compared to traditional methods, as stated in [2]. Motivated by FCN, many networks adopting similar structures were proposed afterwards. These networks use an encoder-decoder structure and apply convolutional layers in the base networks trained for image classification tasks as feature extractors, as mentioned in [3].

Variations of RNN have also become the backbone model of medical image semantic segmentation. U-Net [4] uses the multi-scale learned features in the decoding process and incorporates low level features into the inference in order to achieve a deeper supervision, which is considered critical for improving the segmentation accuracy of medical images [5]. Following

U-Net, V-Net [6] was proposed to process 3D medical image volumes directly, and it introduced the Dice loss function to tackle the label imbalance problem. Moreover, the attention mechanism was integrated into U-Net in [7], which allowed the model to implicitly learn to focus on relevant regions for pancreas segmentation problems.

Even though having greatly enhanced the segmentation accuracy and accelerated the learning process, models built upon FCN still have limitations. As summarized in [8], FCN models perform dense prediction by independently classifying each pixel, through decoding the features extracted by the encoder. However, this independent per-pixel inference scheme sometimes disobeys common visual characteristics. For example, linear classifiers like FCN can predict different labels for similar pixels in the body of the same object as stated in [9]. Moreover, in FCN models, the spatial information loss caused by dimension reduction in the encoding process often leads to the loss of segmentation precision at boundaries between different objects. Conditional random fields (CRFs) are a kind of directionless graphical models that allow the prior knowledge of a good segmentation output to be included in the modeling. By integrating CNN into the segmentation framework, the interactions between pixels can be explicitly modeled, serving as a complement to the linear classifier. Hence, CNN are typically applied as a post-processing tool to enhance the segmentation output produced by FCN models.

1.3 CONTRIBUTION

The development of an advanced brain tumor and attack classification method upon the images of (MRI) is needed utilizing RNN in the deep learning implemented to the image samples of brain. Justifications are provided for choosing RNN as a base technique, which being more extended for straightly supporting the multi-scale classification. That gets the classifier able to classify the tumor and seizures in the images of (MRI) from the dataset.

- Providing a general idea of preceding works and successes upon the brain tumor and seizure classification.
- Applying the approaches of the recurrent neural network (RNN) to the integrated dataset for performing the classification with a lesser amount of data loss and further accuracy.
- Evaluating and comparing the employed recurrent neural network (RNN) in addition to comparing with else investigations from literature.

- Developing an RNN-based novel methodology having virtuous outcomes for the classification of tumor and seizure.
- Which deep learning-based technique is more appropriate for the tumor and seizures classification regarding the accuracy?
- How should the performance of this RNN algorithm be evaluated?

1.4 THESIS STRUCTURE

Chapter one presented the rudimentary features of the key features of the recurrent neural network (RNN) deep learning. And, it introduces the description of the classification of the brain tumor, the interface of the problem statement, where the innovation features regarding the brain being emphasized and certain features concerning the dimensioning. Also, it clarifies the contributions of the principal used cases that consider the facilities and uses anticipated to be reinforced in the classification of brain tumor throughout the metrics of performance, like the needs of the output or the time of response time.

Chapter two explains a complete outlook upon the literature and related works with the overview state-of-the art upon the issues that link to the investigation evolved in this thesis from the academic thesis, the reports of industry, and the research standards.

Chapter 3 describes the highly significant and pertinent models implemented in the simulator. It comprises the taken models and suppositions for the elements of simulator, like detection, segmentation and output computations in addition to the numerology classification inclusion. And, the application of simulator is elucidated in such chapter throughout using the routine inputs and outputs and throughout utilizing the RNN technique workflows in tumor classification. At the termination, an evaluation upon the key elements of simulator is achieved for guaranteeing that the outcomes being useable and right for other investigation.

Chapter 4 characterize the considered scenarios in simulator and the reference factors of the model that considers the detection, propagation models' recognition and classification related metrics, such as the throughput at tumor classification, in which the numerologies being effective among the others, as well as the profile of the reference traffic. From such reference factors, a no. of analyses being conducted from the varied outcomes for studying the influence of various input factors, principally upon the brain, the effective tumors number and the layer's number.

The profile of brain is adapted for studying the influence upon the various classifications of the facility mix share, also the influence upon varying the average output for each tumor classification.

Finally, in chapters five and six, the comparison the debate and main inferences from the simulation outcomes with the else formerly achieved investigations, introducing the highly pertinent and significant outcomes and a concise analysis upon them. Also, certain recommendations for upcoming investigation are offered, depending upon the brain tumor classification still to be unconfined and upon the certain taken key suppositions for the evolution of model.

2. RELATED WORK

In ref. [10], the author suggested the extraction of the tumor from the image via conducting suitable separation methods and geomorphological processes, the correlation being achieved for determining when the extracted tumor can be precisely obtained as tumor. Such regularized cross-correlation has been carried out utilizing the machine learning function. Within such procedure, the extracted tumor with the (MRI) image was compared. When it causes a big positive magnitude (nearby to 1), one knows how to state that the certain cancer is mostly associated with the view. This tumor is extracted capably with a smaller amount of noise. Else, the extracted tumor possesses certain noise in the image owing to which a value of correlation decreases, as mentioned in [11]. Such method of the regularized cross correlation has been implemented upon each segmentation method, with the exception upon the CNN. This is since in the CNN, the MSER characteristics and the plot of the zones depending upon the extracted characteristics employing the (SVM) algorithm were determined. Owing to this, the zone isn't really superimposed upon the initial image. The zone is fair emphasized for displaying the outcome. Therefore, it wasn't likely to calculate the regularized cross correlation for the extracted tumor employing the (DCNN) method. In ref. [12] the superimposition of the zone utilizing the (KNN) technique was also attempted. The ref. [13] wasn't capable to employ the characteristics made from the (MRI) images utilizing the technique of machine learning. Thus, employing the regularized cross correlation, the investigators in ref. [14] obtained that when the extracted tumor possesses certain noise that exists in it or not for the whole segmentation method, with the exception of the (MRI) images.

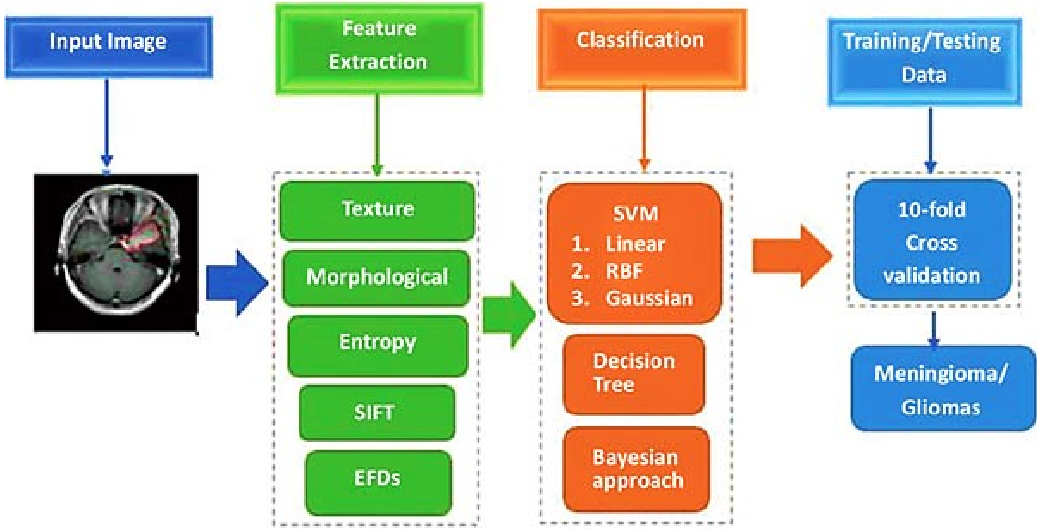

Figure 2.1: THE YOLO9000AN ARCHITECTURE DIAGRAM THAT DEDICATED FOR THE CLASSIFICATION OF VEHICLE [15]

2.1 LITERATURE REVIEW

In such research [16], the researcher utilized the image that's changed to a dual and suitable texture filter technique implemented for determining the image texture characteristics. In this work, the best texture filter determined being the Random Forest method. In ref. [17], the researcher attempted to improve the surfaces of tumor zone (foreground) and skull zone (background), and the smoothing filter was implemented. In ref. [18], the user-defined filter matrix was offered for smoothening the image. The larger the filter size is the better characteristics can be noted. Both the front (tumor) zones and background (skull) zones were extracted employing the (GMM) method. A target changeable vector was prepared completed which comprises 2 classes; Zero for the skull zone, and one for the tumor zone. Currently, the cross correlation is implemented for processing the correlation between the target changeable and tumor zone for determining the level to which the tumor zone pixels being narrowly related with each other. In ref. [19], the cross correlation was calculated utilizing MATLAB. The tumor zone is the values of pixel for the front points unearthed utilizing the Machine Learning from the picture of quality. Like this, the researchers obtained the way the pixels in the tumor zone being narrowly correlated to each other. Nevertheless, once more such cross-correlation value totally relies upon how one chooses the foreground and background points employing the Deep Learning technique. When one doesn't choose the points appropriately; that's for instant, when the tumor zone (foreground) points being regarded at the borders or edges, there's likelihood that one mayn't gain a precise cross-correlation value.

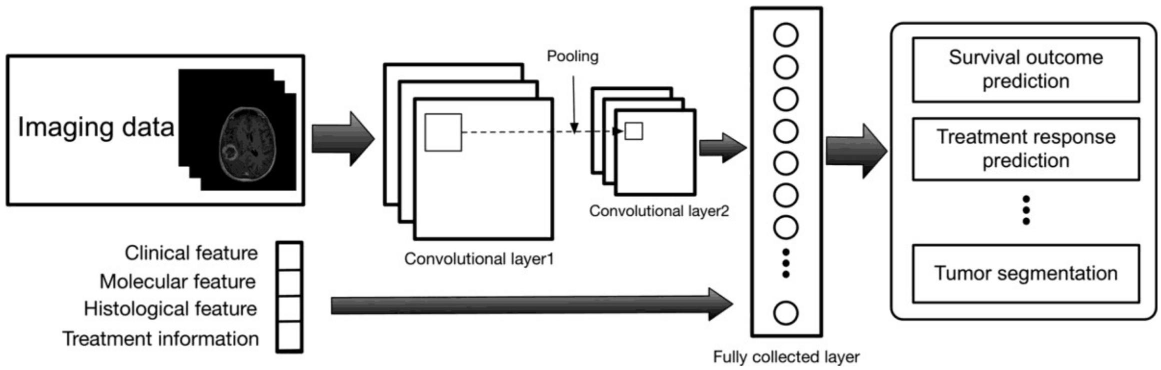

Figure 2.2: The CNN architecture diagram for the segmentation of brain tumor [20]

The researcher in ref. [20] utilized approaches except the (MRI) manages for extracting the tumor properly. And, in comparison to the primary output, one be able to notice some noise in the output. Because of this, the regularized cross over association standards manifested have no tendency. That's due to the incompetent threshold values employed for segmenting the tumor. Also, that's owing to that there's barely every noise observed in the image. Nevertheless, such regularized cross-correlation method isn't implemented upon the tumor created from the (MSER) method. That's due to that in the (MRI), the investigators obtained the (MRI) characteristics and the plot zones founded upon the characteristics extracted employing the Deep Learning methods. Owing to that, the zone isn't really superimposed upon the initial image. The zone is fair tinted for displaying the outcome. Therefore, it wasn't likely to compute the regularized cross-correlation for the extracted tumor employing the (MSER) method. Nevertheless, in ref. [21], the tumor segmentation output being too obvious that via only observing the output, the accuracy can be predicted. To eliminate the noise and show better outcomes, one can choose better threshold magnitudes. As well, in ref. [22], the (MRI) merely portrays a single extracted tumor in place of both tumors. That's caused because of the two potentials. The 1st. being that the range of area offered is lesser which ignores the required image of tumor segment. The second potential is owing to the higher limit magnitude. Thus, in the ref. [23] that is introduced the rise of the range of area and reduction of threshold, the zone of attention can be precisely extracted. In such manner, the needless noise can be removed, and the values of correlation tending toward one being depicted. Nevertheless, in ref. [24], the researchers invented any of segmentation methods; making any variations may cause inaccurate outcomes for certain images and create noisy output for certain images. As well, beyond the extraction of the background and foreground portions of image, the authors have obtained the way the pixels in a tumor zone being narrowly associated to each one via calculating the tumor zone's and the goal variable's cross correlation.

Additional, the author [24] in [25] explained that the correlation coefficient between the target variable and tumor region was originally calculated using feature extraction techniques such as DCT (Discrete Cosine Transform) or GLCM (Gray Level Cooccurrence Matrix). Unfortunately, the idea did not work in this paper as a consequence, I could not apply this principle to my calculation. Those problems may have occurred because of exposure. As a result, the author was able to pull out the foreground and background pixels, and determine the cross-correlation between the texture's features. For regions outside the skull, set the target to 1. This history and foreground points are calculated using deep learning. Also, authors [27,28] used DCNN to extract tumor and skull regions to compute correlation with tumor area The target variable is a human-based, three-specific, three-dimensional representation of the tumor position. The background pixel values in this paper are extracted from the image using Python. This picture has been applied the texture filter and deep learning has been done. Enhancementing the texture in a smoothing filter is applied to the image is described in [31]. how many ways The cross-correlation does, however, hinge on the foreground and background points being selected with the GAN method. If the tumor edges or boundaries are not chosen, such as examples, a faulty cross-correlation will result.

2.2 CHALLENGES OF ONLINE TREATMENT IN WORLD

If the picture is excessively bright, it will be difficult to read the content. As defined in [33], the image is segmented according to the largest/smallest luminance range and threshold. Excessive exposure is dealt with by the segmentation algorithms, resulting in the desired result. As a result, the desired outcomes are not achieved, as demonstrated [33]. Additionally, there are tumors in the areas that have been overexposed. As a result of the tumor zones, the tissue tends to be excessively exposed in [35]. Additionally, this approach is ineffective if the tumor is overexposed. since the predicted tumor cannot be segmented according to the right thresholds These concerns have been raised as a result of the exposure. If we use histogram equalization to adjust the image's exposure, we have a chance of having better results. This image has been processed with a texture filter and deep learning. This measure is used to determine the degree of association between tumor pixels. Comparing segmentation techniques, we evaluated their performance when used in conjunction with LTSM [37]. To determine whether or not the image contains noise, it is compared to the extracted tumor. As a result of the presence of noise, we can conclude that tumor segmentation is incorrect. Otherwise, the tumor's segmentation is aligned with what is observed in.

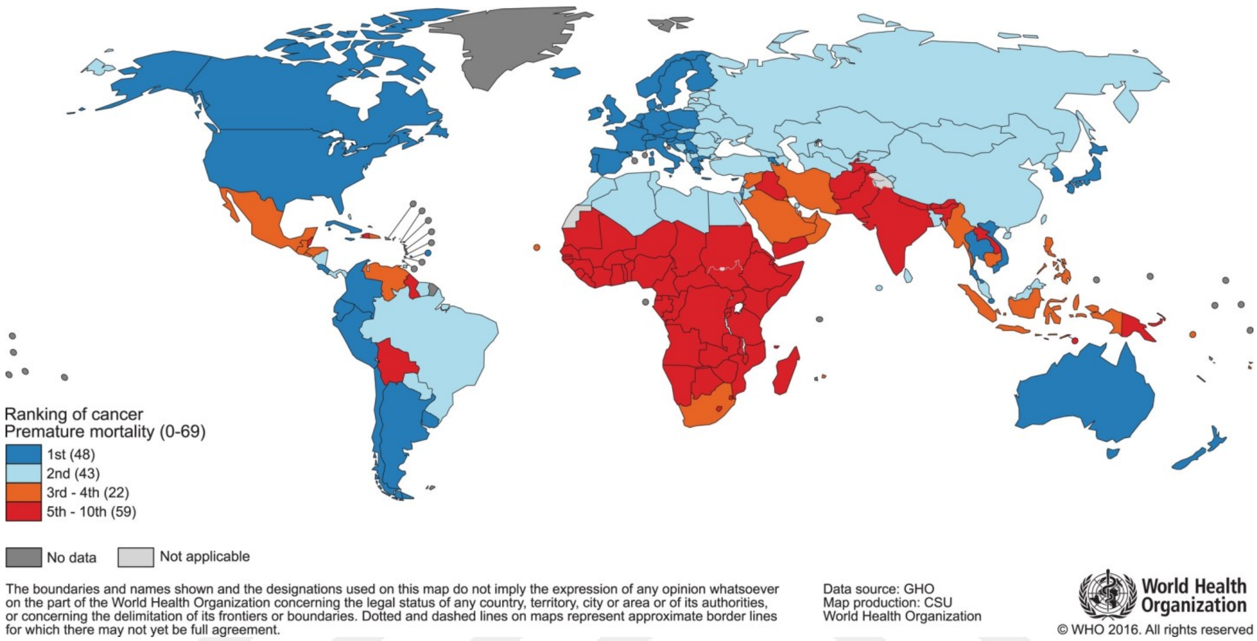

Figure 2.3: Number of brain related diseases cases per 1 million people in different regions of the world according to WHO [39].

2.3 CAPACITY AND COMPLEXITY OF DATA PROCESSING

Since the brain images are all rendered in a [to the range of shades of gray], the result of extracting the values from each pixel of each slice of each brain lesion is zero (0,255] would expand) However, in this particular scenario, the model's output was subpar. This is the explanation; rather than process each image with the data retrieval at the same time, it is unclear how much detail each image has been analyzed by each patient and is treated in a separate manner [since doctors don't bother to find out how long it took], as mentioned in [paraphrased] The data's original distribution was highly variable, which means the data has varied greatly over time, particularly because of continual and varied additions. Areas identical to, with (0,255) the ones in the (1,256) range, (but also can be specified in the ones in-between, for example: 50,150). (-200,8000). However, each lesion value often has a specific minimum and maximum. This does not always mean that the previous lesion values are the lowest and highest, and there could be different minimums and maximums on each affected area (since some slice contains pixel value that is minus which the reason is also not clear). It is critical to note that every block conversion is performed on a different windowing mechanism, which has a noticeable visual impact on each of its displayed slices. In order to solve these problems, all slices have a minimum value of 0 set to them (which is the global initial value), and the limit of each lesion is forced to be equal to the maximum of each processing results. The two given [42] values will be applied to all data slices to cause them to have a value of (0,255) In other words, as well as prior data-slice history for all patients are unified, maximum amount of prior data is carried forward into the next year.

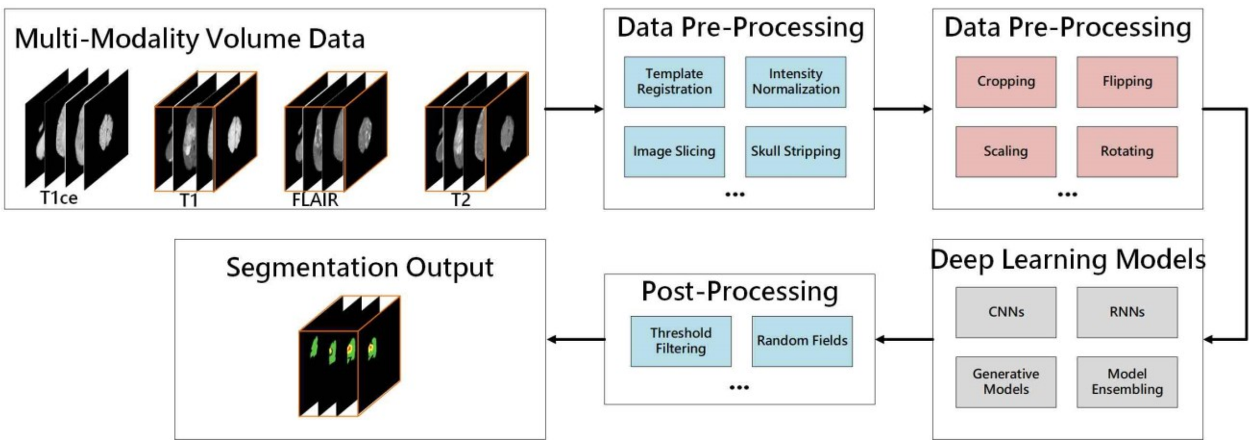

Figure 2.4: The data processing capacity to complexity with the number of samples reduced through the use deep learning model [43].

2.4 CONVOLUTIONAL NEURAL NETWORK

Model based approaches start with a set of hypotheses of the final classification based on rules of the object being classified. For instance, in the case of brain tumor classification a hypothesis can be a particular orientation of the joints. An advantage here is that the hypotheses can be generated from an infinite space of possible classifications. The main difficulty of model-based techniques is that they are often computationally expensive. In addition, model-based approaches tend to be very complex. An example of a model-based technique can be found in [44]. A possible explanation for the observations on the maximum length of the synthetic sequences could come from the class sequence length distribution. While 95% of all original sequences are shorter than 200 frames, there are outlier sequences that are much longer and skew the arithmetic mean class sequence length as given in [45]. As the length of the synthetic samples is based on an CNN distribution that makes use of these statistic, the generator might tend to produce longer sequences that help the classifier to better generalize to these rarer inputs. When clipped, this effect cannot be fully exercised by the generated samples. The smaller the number of training samples, the smaller is the number of original outliers, which increases the positive augmentation impact. Interestingly, the maximum validation accuracy is better for the multi-layer CNN when the synthetic samples are clipped to 100 instead of 200 frames. In this case, the data augmentation emphasizes the inputs that tend to be shorter than the average. Nevertheless, these effects might be rather random statistic correlations and it is unlikely that the positive impact comes from the varying length of the samples alone as mentioned in [46].

Average inter-class, intra-class and centroid distances for the original, generated and combined datasets. The intra-class distances for the best generator loss indicate that the static CNN have learned to produce a wider range of different frames for each class compared to their best inception accuracy counterparts. While the average inter-class distances are also bigger than for the best inception accuracy models, they are still much smaller than for the original training distribution. The FCNN models for brain tumor classification that is very different to each other and thus cause larger average inter- and intra-class distances. The base multi-layer CNN had a positive effect on almost all groups of selected fully connected layers as well as on the complete dataset when used for data augmentation as mentioned in [47]. This is a strong proof that the proposed CNN augmentation method is suitable for improving the classification on brain tumor lesions action sequences. Modifications in the size of the critic architecture led to worse results. While the CNN-augmentation scored higher average best validation accuracy on the complete dataset, it performed worse when tested, showed stability during training and generated sequences of higher visual quality. Thus, without the added gradient penalty term, the CNN appears to be the superior and more stable architectural solution.

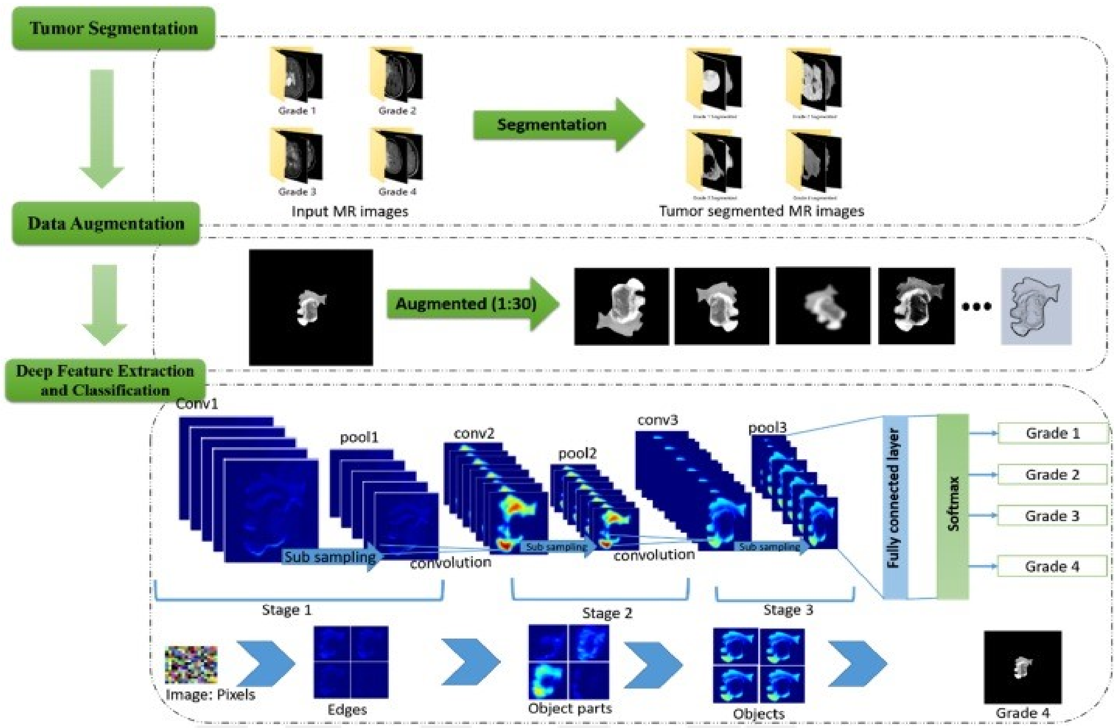

Figure 2.5: The slicing and classification process of brain MRI samples using CNN [48].

2.5 CLASSIFICATION OF BRAIN REGIONS

Classification is the process of separating a given object into different classes. The classification step classifies the extracted and selected features obtained from previous step into different classes. The classification can be both supervised and unsupervised. In supervised method, the features sets are classified into predefined classes while in unsupervised method, the feature sets are assigned to unknown classes as described in [49]. A classifier always requires a training and testing data to train and evaluate the performance of classifier. The data for training in medical images are usually obtained from one or more experts who has assigned labels to a set of objects. Defining Region of Interest (ROI) is the process of separating the desired region or object of interest from the whole background for the further process of feature extraction. ROI in medical images can be defined using both manual or semi-automatic method and automatic method. Manual or semi-automatic method requires user interaction while fully automatic methods is free of user intervention as described in [50]. Generally, a rough image segmentation is performed for defining ROI in medical images. Some of the common methods for defining ROI are thresholding, region growing and boundary tracking, classifier methods, deformable models and atlas-guided methods etc.

Thresholding determines an intensity value either locally or globally to separate the desired object from background. It usually separates the pixels with certain range of intensity as one class and remaining as other class. Though it is simple and a powerful technique, it has its own limitation of inability to take in account of spatial characteristics of image, sensitivity to noise and intensity inhomogeneity [30]. Region growing extracts the connected regions of image based on predefined condition: intensity, image feature etc. [47]. It begins from an initial point called seed point and stops on reaching the stopping criterion. Atlas guided method segments organs using information about the anatomy of interest termed as atlas of anatomy [36]. In this process, the atlas images are transformed using linear, non-linear or a combination of multiple linear or non-linear transformations to real images and segmentation is concerned with determining resemblance between two objects of similar objects. This method is only appropriate when the structures are consistent over slices [38].

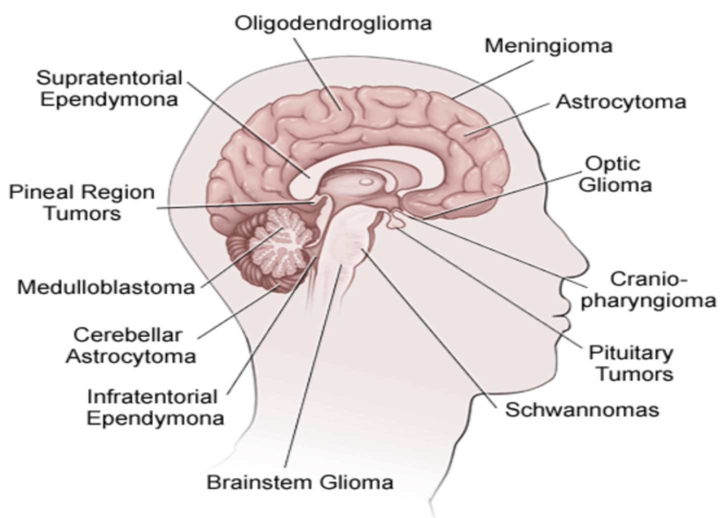

Figure 2.6: Different locations of brain tumor for the automated classification [50].

3. METHODOLOGY

The suggested approach begins by applying various classification methods to the image in order to sharpen the appropriate parts of the image before applying the RNN.

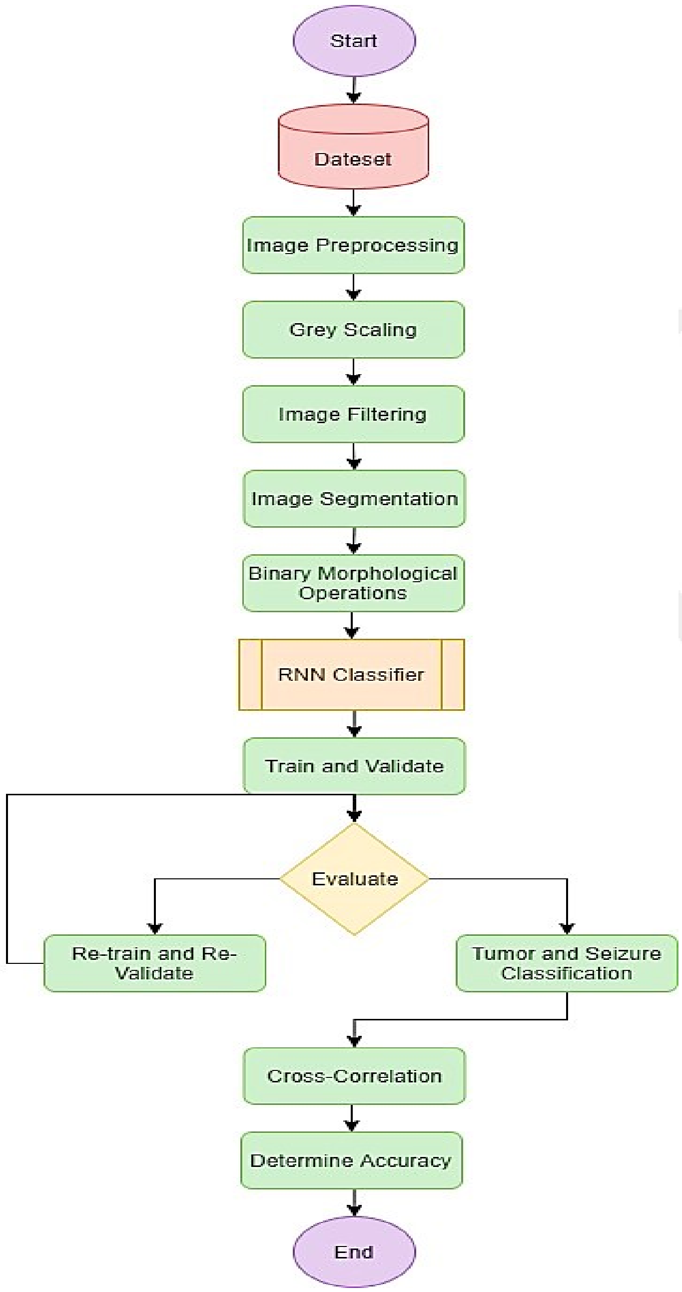

Figure 3.1: Flowchart of approach being followed

The technique was split into several levels. Throughout this development phase, we created distinct modules, each of which was responsible for a distinct mission. We implemented this study in MATLAB R2019a. The following is a brief summary of it:

1. **Implementation Pipeline:** Using the module, the MRI acquisition suite performs on-expansion operations on the raw scans, giving the target regions of interest. Among these are the techniques are the methods of brain localization, region conservation, enhancement, and feature extraction. To ensure that these modules can be applied across the project, we developed them to meet diverse needs. Furthermore, validation exercises often use the same modules as well as those used in data loading, such as the module that pulls data. When searching for brain patterns, the device first employs a few image-based segments for which the approximate probabilities are known. It makes various segmentation images with estimates of brain detection to get an overall sensitivity assessment. the model was developed using the images of the human brain with brain tumor volumes from the experiment known [values of each one particular] as a total of 265 scan. After the model was trained on 200 images from two different groups, it was then applied to 14,000 photos.

2. **Modeling:** We built a corresponding MATLAB module for each RNN learning architecture and MRI-based kernel modeling module, with the open-source deep learning box and hyperpolarized MRI model open-source package. Once these filters are already in place, a wide range of models can be learned: A facility can be created using an integrated MRI device which includes the pre-defined and integrated pre-processing stages. Comparing systems is possible with the addition of this widget. Also, systems that employ this widget are more adaptable when it comes to network construction or modification.

3. **Training and Validating:** To test the viability of the CNN-based learning method, we created two different modules on a 1092 brain image, one to use for training and the other for evaluation. We save qualified models and their related weights to files so that the implementation stage can be validated without launching the testing stage in order to look at them.

3.1 IMAGE PROCESSING PIPELINE

3.1.1 Brain Localization

The guide ensured that the acquisition of MRI training data adhered to the stipulations. After feeding the machine a whole body scan and a small percentage of brain analysis (water-only), the machine's capability was increased and it performed whole body scans before being fed the brain volume based estimate. Additionally, it was fed areas of interest by the operator, which improved the algorithm's effectiveness. The actual coordinates of the brain were determined by rotating the output of the brain scan in the entire body by that number. It has been demonstrated through research that this is valid, indicating that the world coordinate has been changed by the addition of voxel sizes and coordinate system offsets. On the z-axis, the height of a voxel (a.k.a. volume) corresponded to a two-dimensional brain image.

3.1.2 Binary Image Masks

Two binary masks were generated to produce data samples describing regions that are suitable for ROI placement and regions that are not. The brain region mask is focused on the locations of ROIs positioned by the operator. The mask was created by measuring the distance between each ROI and its adjacent ROI. By connecting all ROIs with the shortest distance possible (out of all ROIs), polygons were generated for the binary mask. The polygons were generated using the Algorithm. Each pixel contained within the ROI region was known to contain brain tissue. The mask for the non-brain area was extracted from the image's right-most third section. Here, the likelihood of detecting brain tissue was poor, implying that the region was not part of the brain.

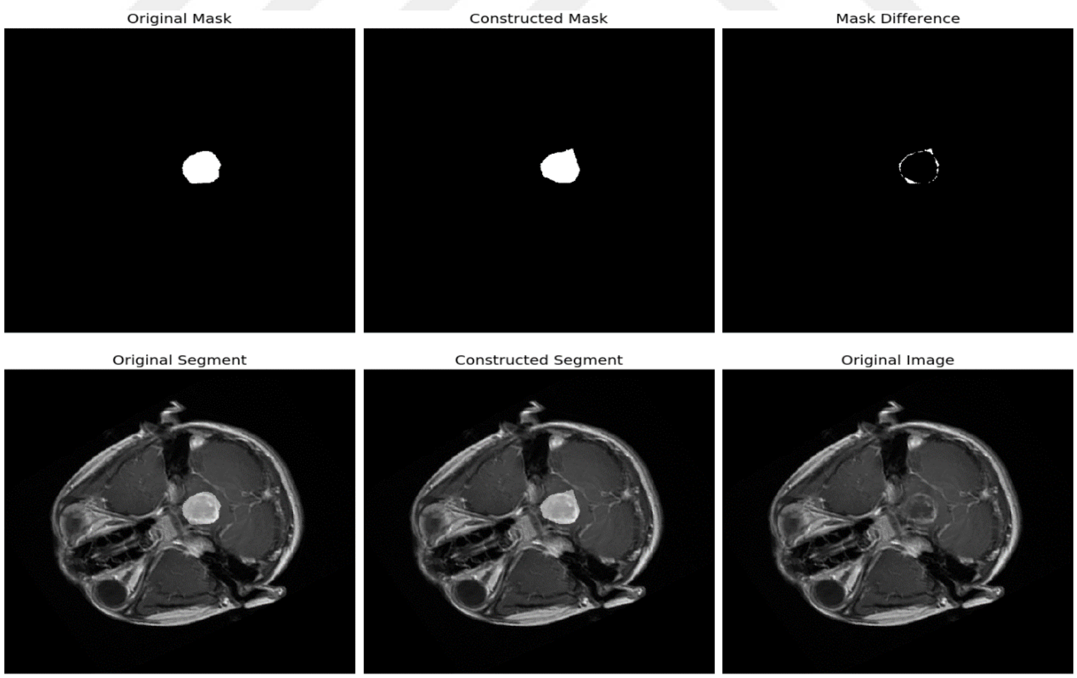

Figure 3.2: The mean mask difference applied on the MRI sample for tumor localization.

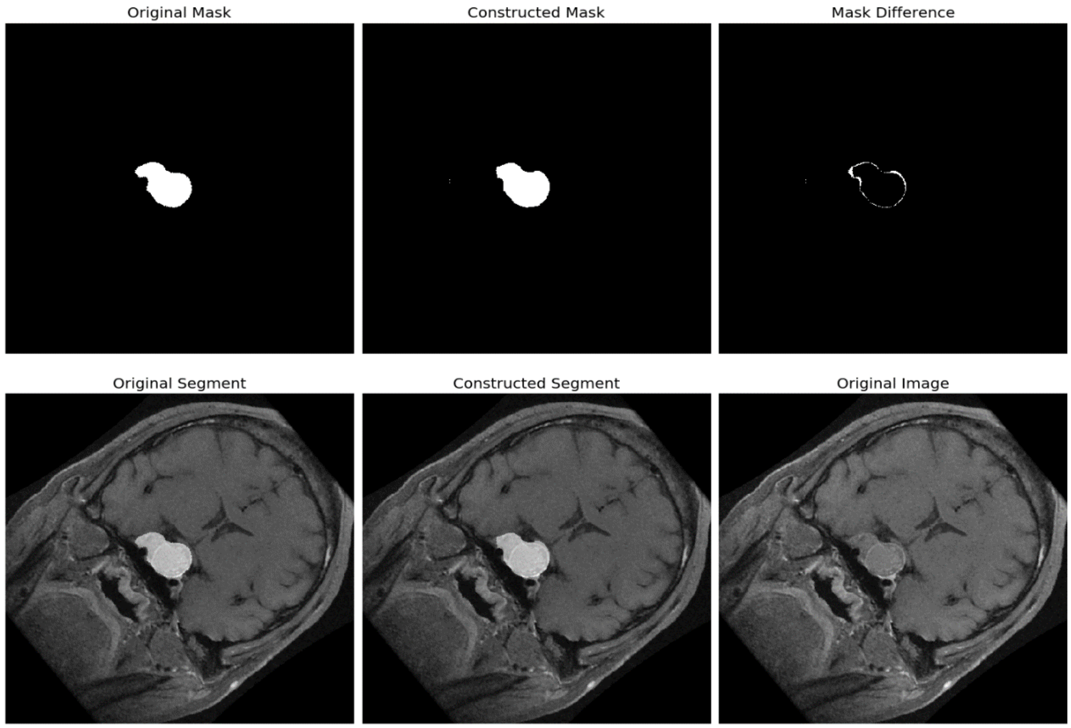

Figure 3.3: The mean mask difference applied on the MRI sample for tumor localization.

3.1.3 Magnetic Resonance Imaging

Magnetic Resonance Imaging, or MRI, is a form of medical imaging. Unlike CT, which uses X-rays or radiation, MRI generates images using a solid static magnetic field, a magnetic field gradient, and radio frequency (RF). The nucleus possesses an inherent property known as spin. As a result of this "spin," the nucleus will develop its own magnetic moment, similar to that of a small magnet. Magnetic resonance imaging (MRI) is the technique that takes advantage of this property. To begin, a strong static magnetic field is used to allow the nucleus to scatter uniformly (parallel or antiparallel to the magnetic field). Due to limited resources at Masters Level, the research is focused on Astrocytoma's gliomas. In future, PHD research, I will consider the Ependymomas and Oligodendroglia's as well. Then, by disrupting the nucleus with RF, a process called precession is caused (the RF frequency should be the same as precession frequency which is related to the static magnetic field). Following the disruption, the magnetic moment gap signal is detected. Additionally, to obtain spatial information, a magnetic field gradient is used, which allows nuclei in different positions to encounter distinct magnetic fields and exhibit distinct magnetic moment variations. Three gradient coils are used to create a three-dimensional representation of the body, one for each of the three axes - X, Y, and Z. The profile of our body can be reconstructed by examining these signals. Today, almost all MRIs employ hydrogen as the target nucleus, as it is a part of water, which accounts for 70% of the brain's volume. The MR image formation process subdivides a section of the patient's body into a set of slices and then each slice is cut into rows and columns to form a matrix of individual tissue voxels. That's due to that in the (MRI), the tissues obtained the (MRI) characteristics and the plot zones founded upon the characteristics extracted employing the RNN method. Owing to that, the zone isn't really superimposed upon the initial image. The zone is fair tinted for displaying the outcome/result.

3.1.4 Feature Extraction

A square Feature Region of Interest (f-ROI) was extracted for each pixel found within the masks. Figure 3.3 illustrates a scale 30 30. The texture and intensity image features mentioned in the background were computed from these regions. A ROI was inserted in each f-ROI inside the brain region mask to determine the region's tumor fat fraction. In most instances, the ROIs were smaller than the f-ROIs. This technique, however, is not used on the tumor produced using the RNN technique. The explanation for this is that in RNN, we define RNN features and plot regions using MATLAB functions. As a result, the area does not appear to be superimposed on the original image. To show the result, the area is simply highlighted. As a result, no normalized cross-correlation could be determined for the tumor and seizures derived using the RNN technique. However, when examining the output, it is clear that RNN produces the best result when compared to other methods.

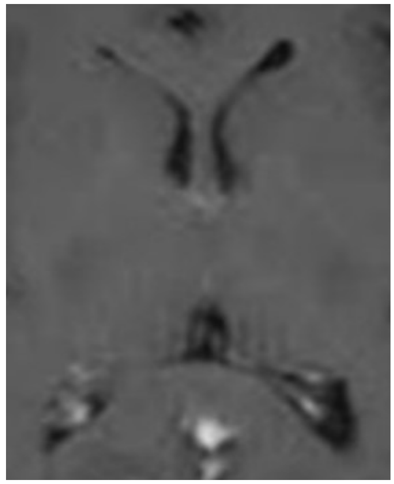

Figure 3.4: A 40 × 40- A tumor's pixel f-ROI was extracted from some kind of MRI Brain images.

Another limitation was that the unit had an approval cap that used only based on ROI classification. percentages that fall within 0.9 points of the company's experience indicated regions and were labeled as acceptable classifications are reported to have adequate long-term stability in all media types tested. unsuitable measurement ranges had negative limits. If a measurement went beyond the lower or upper limit, it was marked as such and assigned a 0. Other regions outside of the brain-mask, outside of both fROIs, were classified as ZERO across all alternative localizers Using a system that used a classifiers and regression models, all the anatomical ROIs on-in-samples belonged to a class mark of 1, which had been correctly marked as a brain area of interest. "Non-Brain Areas" was used for all locations outside the brain masks, where "no brain present" was given a zero classification and other places that lacked an organ designation. There was a high degree of variation between ground truth and predicted active region activity in the regression model training when it came to the fat fraction of the expanded performance predictions. In MRI, the following regions represent the scan of brain which comes under focus. Beyond these extractions of the background and foreground portions of anatomic region, the slices have obtained the way the pixels in a tumor zone being narrowly associated to each one via calculating the tumor zone's and the goal variable's cross correlation for each slice.

- Mastoid region
- Auricular region.
- Occipital region.
- Parietal region.
- Temporal region.

- Frontal region.

3.1.5 Images for Input and Gray Scaling

using a powerful magnetic field (r) to analyze the bodies and major organs, which assists in establishing a picture of the tumor. These MRI images are fed into our processing system, where they are routed across the network to create a data record. In traditional MRI imagery, which is a black-and-white image, MRI images appear as black-and-white images on a computer. However, is it truly a misnomer to refer to it as a misnomer? The amount of red, green, and blue pixels, as well as white pixels, is high in black and white photographs, as black and white only appears on television. Monochrome expansion (M-expansion) becomes more challenging because it must be performed on raw image data rather than on finished image data. As illustrated in the list above, we convert our given image to grayscale, resulting in only white and fully black shades. A filter with the lowest Kelvin setting is neutral gray, whereas one with a higher Kelvin setting is a darker gray. The shaded areas reflect various intensities of the primary colors black, white, red, and blue.

Figure 3.5: An image inserting into the network as well as grey scaling it

3.1.6 Filtering Images

Utilize the median filter to improve the overall image quality and make improvement. Distinguishing important from trivial elements is made simpler when only the relevant data are retained. The median filter is a noise-reduction filter whose primary benefit is that it assists in removing salt and pepper from images. Due to the nonlinear nature of the filter's effect, it operates more slowly than other forms of noise reduction, such as the Gaussian. This implies that the wider the filter, the slower the process expands. We used an automated segmentation method followed by a series of masks that we identified manually and iteratively developed in our research to distinguish the regions of interest in a brain MRI. What is not important to know is omitted; what can produce false findings is omitted; "white areas that are superfluous" are omitted. This would allow us to sort through and classify the image's meaningful portions.

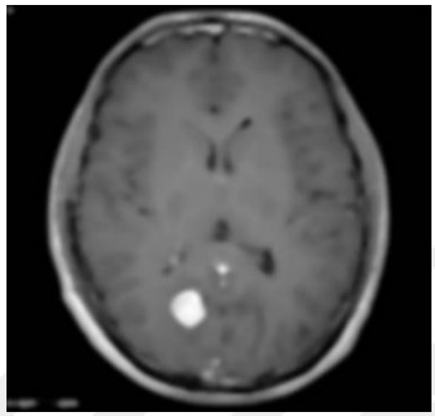

Figure 3.6: Performing the image beyond filtering

3.1.7 Image Segmentation

We can successfully remove the tumor from the image by choosing sufficient segmentation levels. However, this approach sometimes overlooks important portions of the image or finds undesirable portions of the image. As a result, it's possible that only a part of the tumor will be removed, or that some skull regions will be exposed along with the tumor. The displayed regions are entirely dependent on the global threshold values computed by the MATLAB segmentation function.

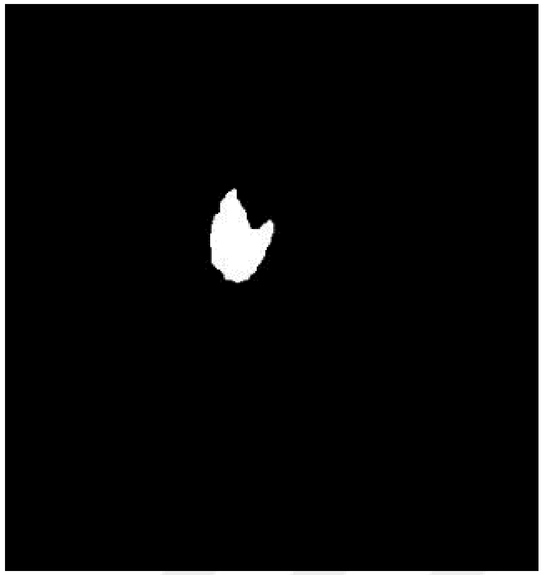

Figure 3.7: The tumor segmentation in a sample of image

3.1.8 Binary Morphological Image Processing

This stage applies enough binary image morphological operations to the segmented area of interest to delete or enhance it. Opening, closing, erosion, and dilation are the morphological operations. Morphological dilation enlarges the area of interest, while morphological erosion removes undesirable clusters created by segmentation. Unwanted regions are removed after segmentation using erosion with a disk size 3 structuring element, while image segmentation is followed by an opening operation involving erosion and dilation.

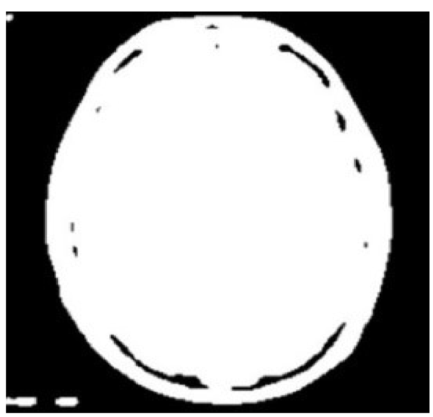

Figure 3.8: Binary morphological processes achieved upon an image

In several cases, Algorithm 1 is the method by which the algorithm acquired data using the same form of data classification. The only distinction was that all regions of a single brain region received equal treatment, with no distinction made between brain and non-brain sections. This technique of iteratively scanning the entire image collection, looking for all possible ROI positions, was extended to all the brain slices. For each position, a gross return on investment (or "ROI") was measured, as well as image features. and then the mean of the feature class was set to a level, namely Mean = 1, and if the ROI was correctly positioned, e.g. Mean = 1, the brain fat concentration was determined. The mean fat fraction was determined by considering the nine regions with the greatest mean and the highest probabilities. The number nine was chosen as a representative number because it is identical to the one used in AMRA's study. A piece of information in the section on brain tumors is defined by the percentage of proliferating brain cells (expanding)

- If $y > 0.5$, Class = 1,
- If $y < 0.5$, Class = 0.

3.2 MODELING WITH RNN

RNN (Recurrent Neural Network) is a form of neural network that has gained popularity in recent years due to its success in a variety of tasks such as object recognition, image segmentation, and object tracking. The connectivity pattern of neurons in the brain was the inspiration for RNN. The main component of an RNN is the convolution process, as the name implies. Convolution is merely a term used in deep learning to describe a method. It is a cross-correlation in mathematics. Convolution is often performed between the kernel (filter) and the image in computer vision applications. The primary goal of these operations is to extract features. RNN needs much less pre-processing than other conventional processes. RNN will learn certain filters that were hand-engineered in conventional methods with enough preparation. The key benefit of RNN is that it eliminates the need to manually extract the matrix and construct the formula to extract the functionality. In feature design, RNN's learnable weights and prejudice are a more efficient alternative to human effort and experience. The basic operation of a recurrent neural network is shown in Figure 3.9.

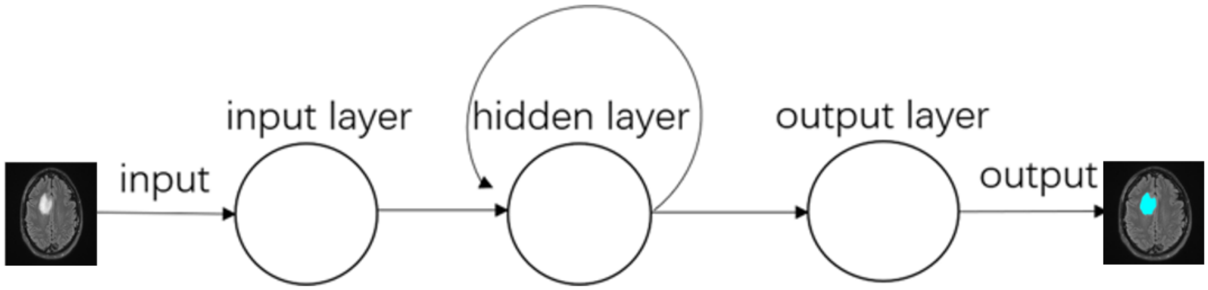

Figure 3.9: Every layer contains a set of functions that are carried out from the source to the destination in order to complete a specific task.

In addition to the convolutional layer, the pooling layer and fully connected layer are two essential types of operations in RNN. Depending on the application, pooling can compute the maximum or average. The pooling layer's goal is to reduce the data's dimension, which may be equal to increasing the receptive field of neurons in the network's later layers. Every neuron in the previous layer is connected to every neuron in the subsequent layer in fully connected layers (FC). It works similarly to a standard Multi-Layer Perceptron (MLP). The FC in the RNN acts as a classifier, categorizing the features obtained in the previous convolutional layers (this is just a rough explanation, in recent works, lots of other methods have been proposed which can replace FC and also achieve a great result). This yields a named matrix with positive integer values for various regions and 0 for ridge lines. Since there is only one catch basin covering the entire picture, this image isn't really useful. Catchment basins are the areas we're looking for. To decide the bright catchment basins that reflect individual regions, we take the complement of our image and add RNN to the complimented image, then negate the gap.

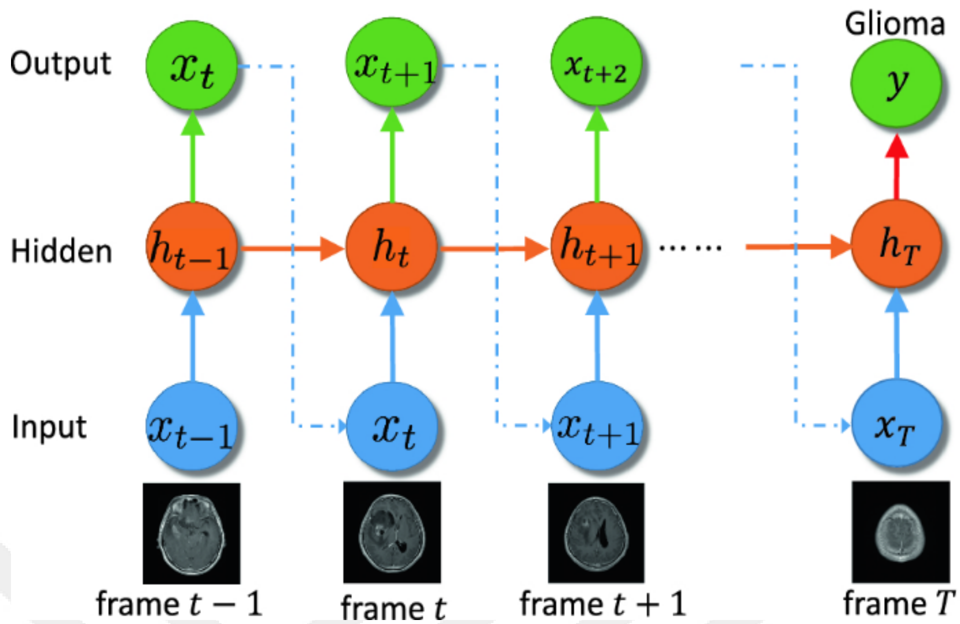

Figure 3.10: The operation of input, hidden and output layer in framing of brain.

Backpropagation often necessitates the incorporation of several individual elements into the network, including the activation mechanism and an augmentation. Recent developments such as dropout, batch normalization, and one-expansion are all proposed, as well as depth-wise convolution and one of the existing innovations. Due to the duration of the paper, an unconstitutional reordering network will not be discussed, as it is only stated briefly in the presentation of the claim. Although some main principles and improvements will be mentioned below, this is not an exhaustive list of the network architecture. Any model is just as good as the one for which you donate all of its data and also includes the additional constraints. For medical images, the primary source of training data is one or more experts who have labeled an item of interest. To begin, the RNN model is trained on the task dataset, which is frequently large and relatively straightforward to collect. After that, the model will be fine-tuned for the task at hand using the dataset. In a RNN the information cycles through a loop. When it makes a decision, it considers the current input and also what it has learned from the inputs it received previously. Tumor is enriched in the RNN layer trees using sub-style plots to distinguish the features that caused this. As anticipated, the MRIs and tissue MRI-derived pixel values are perfectly correlated, showing an absolute correlation between the tumor and the seizure in the image.

3.3 LEARNING WITH RNN

The critical modification needed for this thesis to use the RNN technique is in the final fully connected layer. Given that this is a binary classification problem; the original setting's output number must be changed to one. Additionally, since MRI images differ significantly from general object images and are grayscale, it is important to fine-tune feature extraction methods. The overall strategy is similar to the one seen in the subfigure on the right. Transfer learning is a strategy for moving the training of an RNN model from one task to another. To begin, the RNN model is trained on the task dataset, which is frequently large and relatively straightforward to collect. After that, the model will be fine-tuned for the task at hand using the dataset. This technique is advantageous when data collection is difficult, as it is in medical applications. One of the most important advantages of deep learning methods is their rapid implementation. Although deep learning methods require significantly more time to train on MRI image samples than conventional machine learning methods, their total time cost in this thesis, including data preprocessing, is actually less. According to the theory, the manual feature extraction process takes too long since the features of each pixel are extracted individually. Although the situation would inevitably improve if a more effective feature extraction method is used, this advantage occurs in this case and will occur in others. If the training is complete, the gain becomes even more apparent, and the time cost is reduced to testing.

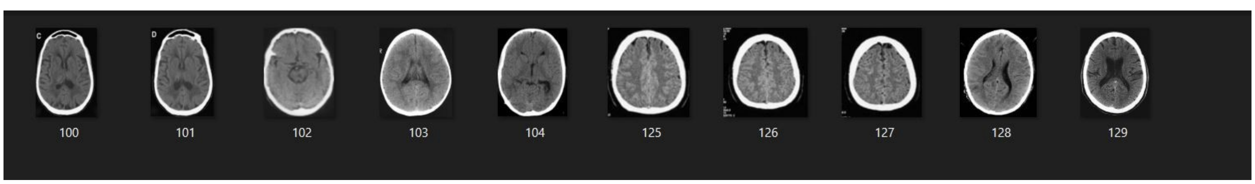

Figure 3.11: For brain MRI samples, an RNN schematic diagram is shown. For the conversion and equal prediction operations, there are various discriminators and generators. Only right samples are retrained for learning in this study. Apart from the extracted samples, we also use the RNN method to fine-tune the function extraction.

3.4 TRAINING AND VALIDATION

To train and optimize the RNN-transfer learning model, the adaptive RNN optimization algorithm included in MATLAB R2019a's Deep Learning Toolbox was used. Suitable and undesirability was examined/m random acquired training data were all used to achieve a comparable percentage of unsuitable and suitable areas Data were double-checked to ensure no duplicates were present prior to reaching the desired level of balance to eliminate skewness, the data were transformed to have a mean of zero and a standard deviation of one. To expand the whole system by its mean and by the system's variance, each function was multiplied by the sum of the other functions and then divided by their sum. The model was then fitted to the data until no additional valuable fitting parameters were found that would yield a further decrease in the loss function value was found. The model was tested up to 100 epochs using 200 reliable 65 examples to ensure that it produced accurate results. We also use current and innovative technology to arrive at the most accurate result. Moreover, to address the problem of focal misregistration in medical imaging, we implement object detection techniques as part of our semantic segmentation process to classify ROIs and perform local segmentation method. Given the additional level of supervisory attention during this stage of segmentation, the networks' preparation, the segmentation networks undergoes refinement.

```
Using Ubuntu 16.04 LTS with CPU Intel i7-6500 3.20GHz, GPU GeForce GTX1080, DRAM 16GB
Train on 200 samples, validate on 65 samples
Epoch 10:
1092/1092 - 305s - loss: 0.612 - acc: 0.9731 - val_loss: 0.015 - val_acc: 0.724 Epoch 20:
1092/1092 - 305s - loss: 0.193 - acc: 0.9917 - val_loss: 0.189 - val_acc: 0.9937 Epoch 40:
1092/1092 - 306s - loss: 0.135 - acc: 0.9939 - val_loss: 0.225 - val_acc: 0.9941 Epoch 60:
1092/1092 - 306s - loss: 0.086 - acc: 0.9967 - val_loss: 0.237 - val_acc: 0.9934 Epoch 80:
1092/1092 - 306s - loss: 0.079 - acc: 0.9969 - val_loss: 0.194 - val_acc: 0.9940 Epoch 100:
1092/1092 - 306s - loss: 0.063 - acc: 0.9975 - val_loss: 0.221 - val_acc: 0.9937
Dice Co-efficient:
Brain co-eff = 0.990807830811   auc = 0.990807830811   sensitivity = 0.990807830811
Sensitivity:
Tumor co-eff = 0.969423287535   auc = 0.940785339355   sensitivity = 0.999859480348
```

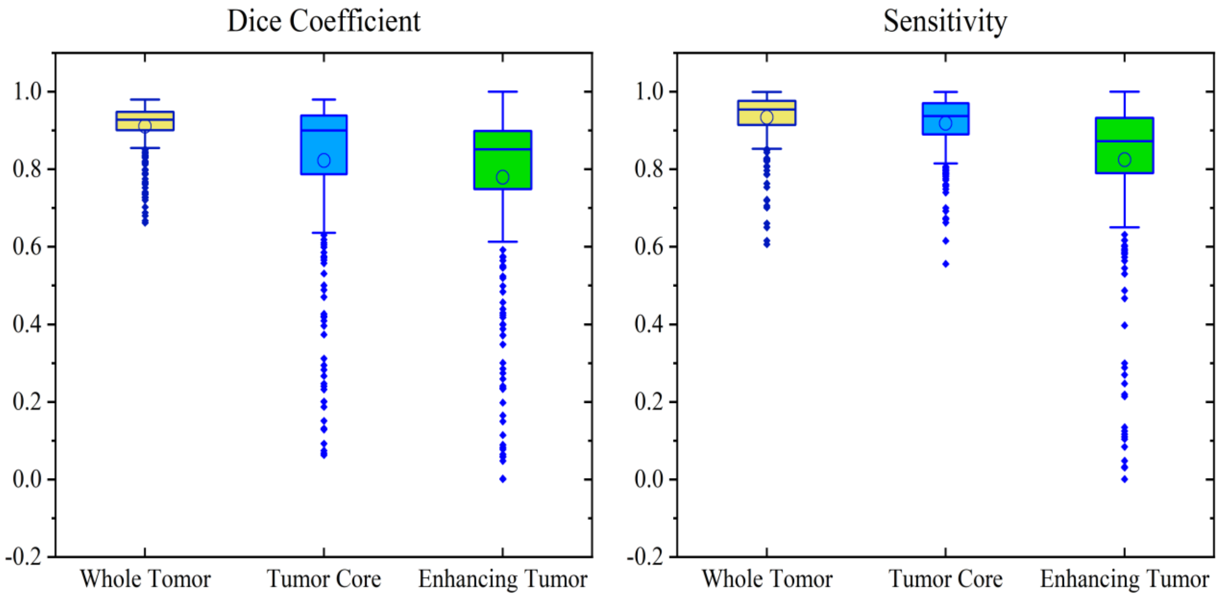

Figure 3.12: RNN model accuracy in terms of training on 100-epochs

Epoch	*Training Loss*	*Training Dice Score*	*Validation Loss*	*Validation Dice Score*
0	1.000	0.134	0.732	0.248
15	0.433	0.598	0.413	0.580
30	0.386	0.651	0.421	0.575
45	0.356	0.676	0.393	0.594
60	0.324	0.792	0.349	0.642
75	0.295	0.816	0.361	0.630
100	0.182	0.929	0.352	0.644

Table 3.1: RNN model accuracy in terms of training and validation on different epochs.

4. RESULTS

Although the RNN generates appropriate results for all pictures, this one clearly outperforms the others. Tumor segmentation and thresholding employ the use of white-colored cells to identify the tumor area on an image. The tumor is depicted in blue on an MRI image, contained in a gray region, and nondivergent or suppressed in a darker area. Tumor is enriched in the RNN layer trees using sub-style plots to distinguish the features that caused this. As anticipated, the MRIs and tissue MRI-derived pixel values are perfectly correlated, showing an absolute correlation between the tumor and the tumor in the image. Due to the absence of grain in the picture, it produces almost no noise. However, it should be noted that this approach is not applicable to tumors produced using the RNN technique. The explanation for this is that RNNs utilize features and regions specified in the Matlab function used to plot them; thus, we are attempting to use them. The expansion has been removed to emphasize the region's superimposition on the original picture. This section of the region is illustrated to illustrate the influence. However, since the data used by the RNN could not be extended, normalized cross-correlation could not be measured. When compared to other approaches, the results indicate that RNN produces the best results for all the data. The proposed RNN method accomplishing 99.71% accuracy for classifying all the tumors and seizures in sample images. The results of the brain tumor classification task evinced that the proposed formulated automated RNN can effectively enhance the classification accuracy. The results of the brain tumor segmentation task strengthen this enhancement and elucidate that the overall performance produced by combining the formulated RNN post-processing and the lesion localization is better than the conventional methods.

Then, we performed a cross-correlation on the seizure and tumor regions to identify regions in which the pixel values significantly differ from the target variable in an image, and then calculated the degree to which the pixels in those regions are related. The tumor area contains values extracted manually using Matlab functions, while the target area contains values. The tumor and seizure regions, as well as the skull area, are drawn using this neural network technique. The foreground and background points are extracted from the texture-filtered image using Matlab commands. The operating system was set to Ubuntu 16.04 LTS for training and testing, and an Intel i7-6500 CPU, NVIDIA GeForce GTX1080 GPU, and a total of 16GB of DRAM were used. MATLAB was our preferred software development environment.

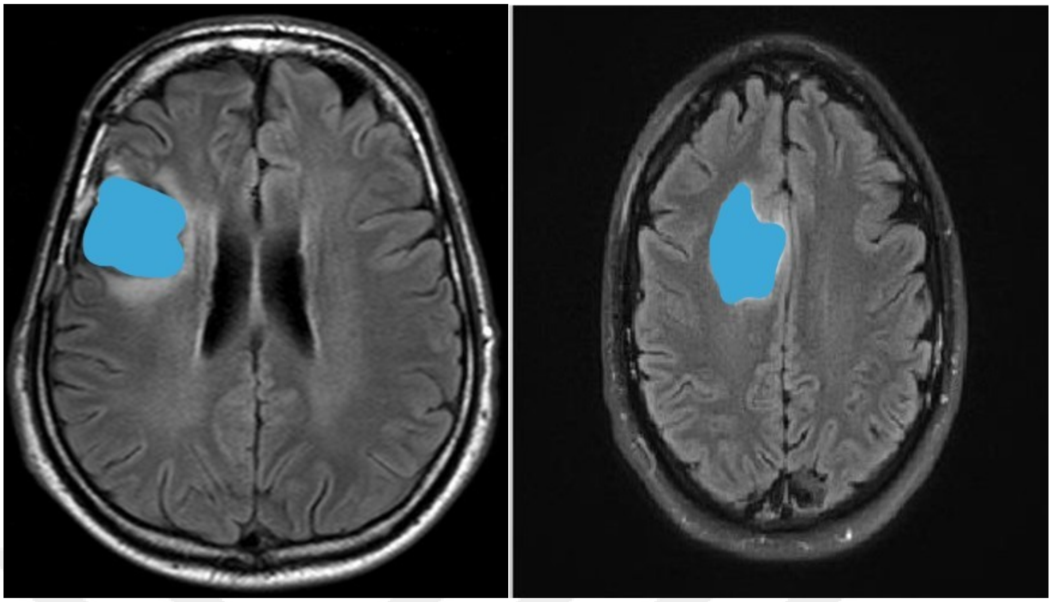

Figure 4.1: Brain tumor classification from the MRI image sample utilizing the RNN method

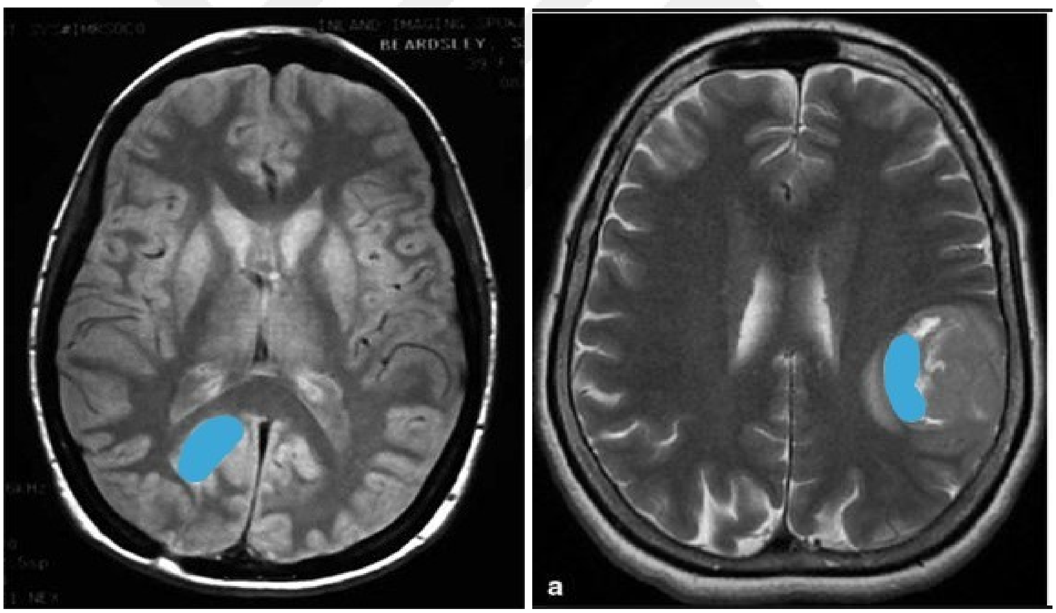

Figure 4.2: Brain tumor classification from the MRI image sample utilizing the RNN method

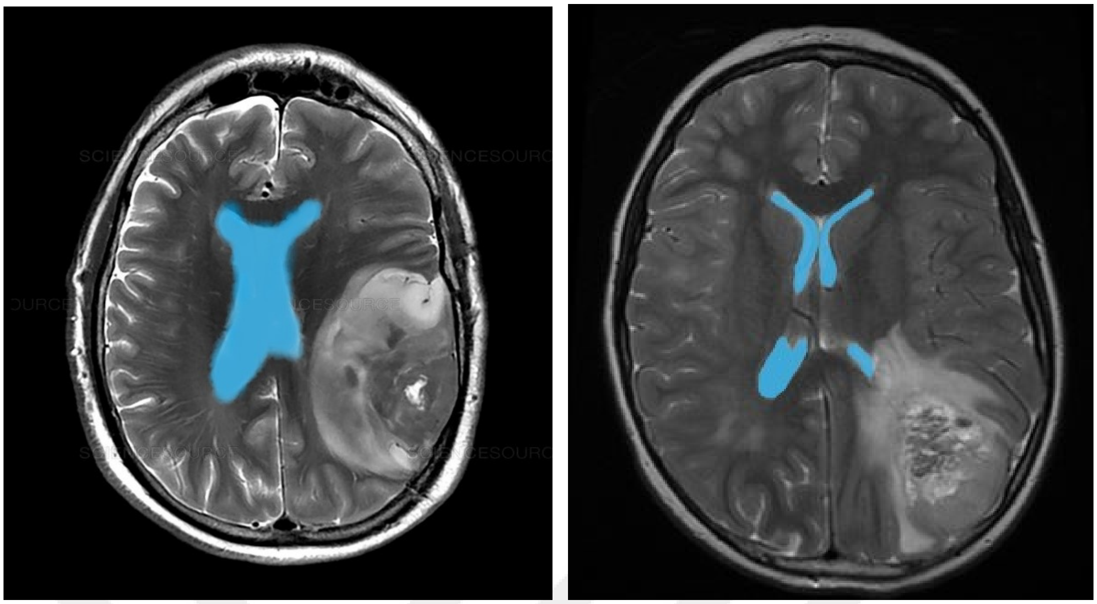

Figure 4.3: Brain seizure classification from the MRI image sample utilizing the RNN method

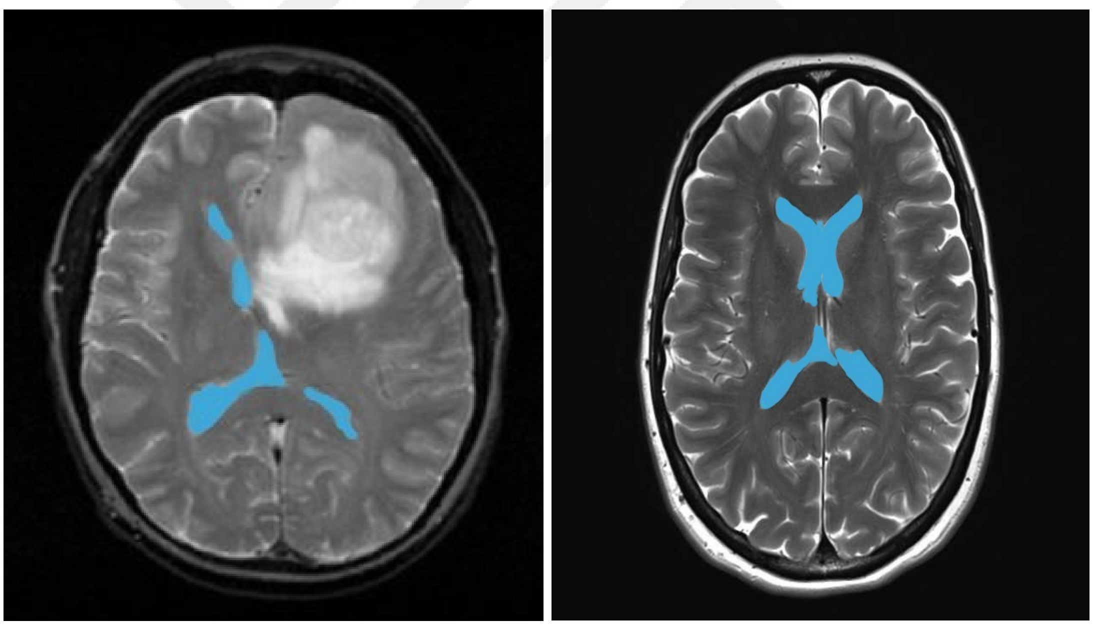

Figure 4.4: Brain seizure classification from the MRI image sample utilizing the RNN method

Essentially, the thesis' objective is to develop a model that is simple to implement and apply to gadoxate-supple MRI data. This study demonstrates that using the same MRI data, different class models can yield very promising results, and it also provides a general procedure for others to follow to learn how to create their own class models. This method is better since a recipe will include only certain values, which, rather than variables, the company can manipulate to meet their unique needs. Due to the model's large differences, this approach would require the model to be re-expanded to fit them. Rather than training individual models, the correct approach in this case would be to decide which procedures or features are effective at classification and then allow each team to create their own model to meet their specific needs.

Deep learning strategies provide significant benefits in terms of training speed, including a more robust training capability and a shorter training period. Although it is true that machine learning methods take slightly longer to train on MRI images than on normal images, the processing and serving of data prior to the start of the training is significantly faster. It is also true that machine learning methods take less time overall than conventional models. Experiment with the hypothesis: The manual process extracts features for each pixel and is believed to be slower than the automated process. This is advantageous because it does not work well when combined with a more efficient feature extraction technique; the functionality of this feature is inferior to that offered by the other technique but remains. If the preparation is finished, the advantages become apparent. Training is ineffective if the cost of testing does not decrease over time.

A significant issue must be investigated to decide if a deep learning model solution is the best option to use and to collect adequate training data for neural network-based tumor analysis. To classify these areas, studies had to be conducted with a particular emphasis on the following:

This was not included in the analysis because it lacked tumors. R.O.I.

Is it significant that images have differing requirements for ROI scale, even more so when separate requirements exist for brain tumor detection and extraction? The findings from these trials indicate that further research on different sizes is necessary to fully understand the magnitude of the effect.

Is the RNN estimation technique precise enough, or do tumor volumes need to be considered? It was observed by comparing automated and manual measurements.

It was discovered that by separating validation and input data in training and validation data groups, the method becomes significantly simpler. Additionally, there were examples of a tumor that was located inside the brain, a tumor that was not suitable for brain penetration, and a tumor that was located outside the brain. The accuracy of this classifier's mathematical calculations as a set of data grows in abundance over time is at least adequate for the tasks in the class assignments. The loss column contains the final value of the squared error function; the effects are detailed in the Squared loss. Caution should be exercised in correcting any minor textual errors that might exist. This was attributable to ROI false positives in inconvenient locations and unresectable tumor areas, as well as a scarcity of targetable lesions. Additionally, this explains why the ROI distributions in brain tumor tissue were too small, resulting in the incorrect tumor values.

5. DISCUSSION

5.1 DISCUSSION

RNNs are an important method for image classification, as shown by the results. Just 65 images from the dataset were used to evaluate the proposed classification using RNN technique. These photos were taken in a variety of lighting conditions and from various angles. Normalized cross-correlation was also used to assess the tumor extraction's efficacy. That is, if the tumor extracted contains noise, the correlation value would not tend to 1. The value would be close to 1 if this is not the case. Except for RNN, all segmentation strategies use this normalized cross correlation. To determine how closely the pixels of the tumor region are correlated with each other, cross correlation was computed between foreground and background pixels of the texture function extracted image. Each technique has its own set of disadvantages, and it may or may not function for some pictures. When compared to other segmentation techniques, the RNN technique for classifying the tumor produces the best results for the tumor region for the area range and segmentation value defined in most of the images. This method, however, fails for certain images with multiple tumor regions, images with very small tumor regions, or images that are overexposed. This issue arose as a result of an incorrect threshold value or area range. One can increase the efficiency of this method by using appropriate pre-filtering techniques and choosing appropriate parameters to detect the features.

ARTICLE	TECHNIQUE	ACCURACY
[51]	Feed-Forward Neural Network	99.00%
[52]	K-Nearest Neighbor	96.90%
Proposed	Recurrent Neural Network (RNN)	99.71%

Table 5.1: The proposed technique is compared to other methods**.**

This study is deemed essential in order to develop a completely automated system for brain tumor classification. Below are several suggestions for areas that should be researched further in order to develop the methods mentioned in this study. For starters, since the Kaggle-based Brain MRI Tumor detection dataset has more data, tests with greater quantities of data should be run to achieve higher statistical correctness. A more precise study of the suggested methods should be possible with larger data sets. It would be important to increase the number of gray value statistical features because strength features produce high scores without any textural features. Intensity histograms, for example, can be used to describe intensity distributions in greater detail.

This enhanced brain segmentation removes tumor classification errors outside the brain. We established a better approach that involves eliminating false tumor classifications from the right side of the picture, which is where the brain is most often found. The RNN technique is used to test more complex and accurate methods. We developed a fully automated brain tumor measurement system based on RNN and MRI, and there are only a few shortcomings that need to be addressed in this thesis, namely the ability to automatically locate the brain location in a whole-body MRI scan. Since the tested textural features achieved such positive results within the brain and in the classification of brain tumor tissue, they should also suffice in locating the brain, or at the very least be a useful starting point for future research.

The most significant advantage of the RNN deep learning technique for brain tumor identification and classification over the manual approach was that the acceptance limit parameter did not need to be set to a particular value to obtain better results. Furthermore, in some cases, the ROIs were inserted in the spleen, resulting in a calculation of the brain tumor fraction that was ahead of the curve. According to the RNN deep learning technique for brain tumor classification on MRI images, accurate brain segmentation was not needed to produce results comparable to manual measurements, but it could improve performance in some cases.

6. CONCLUSION

6.1 CONCLUSION

To review, this study focuses on segmenting brain tumors from MRI images and computing normalized cross-correlation between the extracted tumor and the MRI image. This value measures the degree of precision of the extracted tumor and seizures and lets us assess whether there is any noise present in the tumor extracted. MATLAB is often used to remove the foreground and background pixels from the texture image. The tumor pixels are in the foreground, and the skull pixels are in the background. Using image processing and the RNN technique, cross-correlation is computed between the target variable vector and the tumor region to determine how pixels in the tumor region are closely connected, with an accuracy of 99.71 percent. The pixel values for the foreground points derived from the texture image using the RNN technique are represented by the tumor and seizure regions. Based on the importance of correlation, we were able to assess the amount of noise present in the picture of the segmented tumor using the RNN technique. If the value is approaching one, the tumor and seizures derived are right and precise.

6.2 FUTURE RECOMMENDATION

There is always plenty of room for improvement and testing. Perhaps doctors will continue to use biopsy as the gold standard in the near future, but these picture methods can be used to detect a brain tumor at an early stage in a relatively simple process, or to serve as a second reference standard for doctors to see if the gold standard is truly effective.

- Since, as previously stated, biopsies can often go wrong. It's always helpful to have another staging guide that doesn't cost a lot of money.

- The ultimate aim is to replace the invasive staging process, and as previously stated: The aim of this study is not to provide a model or formula that anyone can pick off the shelf and insert into their data set; rather, it is to find out a technique or set of features that could be used to stage brain tumors on any MRI data set using Brain Images.

- The advancement of computer vision techniques now does not allow for a single model to match every data set, which might never be possible given the wide range of MR imaging methods.

- The RNN features combined with the LTSM model have been shown to be useful for classifying brain tumors in the original deep learning process.

- The deep learning approach, on the other hand, demonstrates that transfer learning is effective and that the model converges quickly (with only 50 epochs of training).

- It also demonstrates that, with proper data augmentation, a large number of individual patient data does not appear to be needed to produce a satisfactory result.

- Even though the conclusion of this study indicates that a large amount of data is not required for preparation, more data is required for testing. Currently, the amount of data used for research is insufficient, resulting in our model's reputation being lowered.

- In addition, more data is needed to train a model that can distinguish and stage from the others. The models developed in this thesis are only intended to distinguish brain tumors from other types of tumors; however, having a model that can determine the exact tumor stage is necessary for real-world medical applications, and can also be a powerful tool for detecting brain tumors at an early stage.

- It is difficult to collect more data in a medical application, so collaborating with other hospitals is a safer option. It would be easier to build a useful model if data and information are shared. This thesis is just the beginning of a project to develop a brain tumor classifier based on MR images, and further work will be needed in the future to develop a fully functional device.

REFERENCES

[1] Anandan, P. and Sabeenian, R.S. (2016) Medical Image Compression Using Wrapping Based Fast Discrete Curvelet Transform and Arithmetic Coding. Circuits and Systems, 7, 2059-2069

[2] Li, Y.C., Yang, Q. and Jiao, R.H. (2010) Image Compression Scheme Based on Curvelet Transform and Support Vector MAchine. Expert Systems with Applications, 4, 3063-3069

[3] Geethu Mohana, M. Monica Subashini, "MRI based medical image analysis: Survey on brain tumor grade classification", Biomedical Signal Processing and Control 39 (2018) 139–161M. Young, The Technical Writer's Handbook. Mill Valley, CA: University Science.

[4] Eman Abdel-Maksoud et al, "Brain tumor segmentation based on a hybrid clustering technique", Egyptian Informatics Journal (2015) 16, 71–81

[5] Shin Hoo-Chang et al., "Deep Convolutional Neural Networks for Computer-Aided Detection: CNN Architectures, Dataset Characteristics and Transfer Learning", IEEE Trans Med Imaging. 2016 May; 35(5): 1285–1298

[6] A. R. Abdulraqeb et al., "An Automated Method for Segmenting Brain Tumors on MRI Images", Biomedical Engineering, Vol. 51, No. 2, July, 2017, pp. 97-101.

[7] H C Sateesh Kumar et al., "Automatic Image Segmentation using Wavelets", IJCSNS International Journal of Computer Science and Network Security, VOL.9 No.2, February 2009, PP: 305-313.

[8] K.A.Helini Kulasuriya et al., " Forecasting Epileptic Seizures using EEG signals, wavelet transform and Artificial Neural Networks" 978- 1-61284-704-7/11/$26.00 ©2011IEEE, pp557-562

[9] Gurbinder Kaur, Balwinder Singh, "Intensity Based Image Segmentation Using Wavelet Analysis and Clustering Techniques" Indian Journal of Computer Science and Engineering (IJCSE), Vol. 2 No. 3 Jun-Jul 2011,379-384.

[10] Wang, G.; Zuluaga, M.A.; Pratt, R.; Aertsen, M.; Doel, T.; Klusmann, M.; Ourselin, S. Slic-Seg: A minimally interactive segmentation of the placenta from sparse and motion-corrupted fetal MRI in multiple views. Med. Image Anal. 2016, 34, 137–147

[11] James S. Walker (2006) Wavelet-based image processing, Applicable Analysis, 85:4, 439-458, DOI: 10.1080/00036810500358874

[12] A. Sindhuja,V. Sadasivam, “Wavelet Based Segmentation Using Optimal Statistical Features on Breast Images”, ICTACT Journal On Image And Video Processing, May 2014, Volume: 04, Issue: 04, Pp:853-857.

[13] Priyadarsan Parida, Nilamani Bhoi, “Wavelet based transition region extraction for image segmentation”, Future computing and Informatics Journal 2(2017) 65-78.

[14] Heba Mohsen et al., “Classification using deep learning neural networks for brain tumors”, Future computing and Informatics Journal 3 (2018) 68-71

[15] Available Online: https://www.eurekaselect.com/node/163868/article/detecting-brain-tumor-using-machine-learning-techniques-based-of-different-features-extracting-strategies

[16] Ali ARI, Davut HANBAY, “Deep learning based brain tumor classification and detection system”, Turkish Journal of Electrical Engineering & Computer Sciences”, (2018) 26: 2275 – 2286.

[17] Long, J.; Shelhamer, E.; Darrell, T. Fully convolutional networks for semantic segmentation. In Proceedings of the IEEE Conference on Computer Vision and Pattern Recognition, Boston, MA, USA, 7–12 June 2015; pp. 3431–3440.

[18] Zheng, S.; Jayasumana, S.; Romera-Paredes, B.; Vineet, V.; Su, Z.; Du, D.; Torr, P.H. Conditional random fields as recurrent neural networks. In Proceedings of the IEEE International Conference on Computer Vision, Santiago, Chile, 7–13 December 2015; pp. 1529–1537.

[19] Liu, Z.; Li, X.; Luo, P.; Loy, C.-C.; Tang, X. Semantic image segmentation via deep parsing network. In Proceedings of the IEEE International Conference on Computer Vision, Santiago, Chile, 7–13 December 2015; pp. 1377–1385.

[20] M. Zhou, J. Scott, B. Chaudhury, L. Hall, Radiomics in Brain Tumor: Image Assessment, Quantitative Feature Descriptors, and Machine-Learning Approaches, American Journal of Neuroradiology Feb 2018, 39 (2) 208-216; DOI: 10.3174/ajnr. A5391

[21] Havaei, M.; Dutil, F.; Pal, C.; Larochelle, H.; Jodoin, P.-M. A convolutional neural network approach to brain tumor segmentation. BrainLes 2015, 2015, 195–208.

[22] Pereira, S.; Pinto, A.; Alves, V.; Silva, C.A. Deep convolutional neural networks for the segmentation of gliomas in multi-sequence MRI. BrainLes 2015, 2015, 131–143.

[23] Kamnitsas, K.; Ledig, C.; Newcombe, V.F.; Simpson, J.P.; Kane, A.D.; Menon, D.K.; Glocker, B. Efficient multi-scale 3D CNN with fully connected CRF for accurate brain lesion segmentation. Med. Image Anal. 2017, 36, 61–78.

[24] Alanazi, H.O.; Zaidan, A.A.; Zaidan, B.B.; Kiah, M.L.M.; Al-Bakri, S.H. Meeting the security requirements of electronic medical records in the ERA of high-speed computing. J. Med. Syst. 2015, 39, 165

[25] Yi, D.; Zhou, M.; Chen, Z.; Gevaert, O. 3-D convolutional neural networks for glioblastoma segmentation. arXiv 2016, arXiv:1611.04534.

[26] G. Palozzi, Binci, D.; Appolloni, A. E-health and co-production: Critical drivers for chronic diseases management. In Service Business Model Innovation in Healthcare and Hospital Management; Springer: Berlin, Germany, 2017; pp. 269–296.

[27] Sparks, R.; Celler, B.; Okugami, C.; Jayasena, R.; Varnfield, M. Telehealth monitoring of patients in the community. J. Intell. Syst. 2016, 25, 37–53.

[28] Ari, A.; Hanbay, D. Deep learning based brain tumor classification and detection system. Turk. J. Electr. Eng. Comput. Sci. 2018, 26, 2275–2286.

[29] Usman, K.; Rajpoot, K. Brain tumor classification from multi-modality MRI using wavelets and machine learning. Pattern Anal. Appl. 2017, 20, 871–881.

[30] Pereira, S.; Meier, R.; Alves, V.; Reyes, M.; Silva, C. Automatic Brain Tumor Grading from MRI Data Using Convolutional Neural Networks and Quality Assessment. In Understanding and Interpreting Machine Learning in Medical Image Computing Applications; Springer: Berlin/Heidelberg, Germany, 2018; pp. 106–114.

[31] Pashaei, A.; Sajedi, H.; Jazayeri, N. Brain Tumor Classification via Convolutional Neural Network and Extreme Learning Machines. In Proceedings of the 2018 8th International

Conference on Computer and Knowledge Engineering (ICCKE), Mashhad, Iran, 25–26 October 2018; pp. 314–319.

[32] Afshar, P.; Mohammadi, A.; Plataniotis, K.N. Brain Tumor Type Classification via Capsule Networks. In Proceedings of the 2018 25th IEEE International Conference on Image Processing (ICIP), Athens, Greece, 7–10 October 2018; pp. 3129–3133.

[33] Kurup, R.V.; Sowmya, V.; Soman, K.P. Effect of Data Pre-processing on Brain Tumor Classification Using Capsulenet. In International Conference on Intelligent Computing and Communication Technologies; Springer Science and Business Media LLC: Berlin/Heidelberg, Germany, 2019; pp. 110–119.

[34] Srinivasan, K.; Nandhitha, N.M. Development of Deep Learning algorithms for Brain Tumor classification using GLCM and Wavelet Packets. Caribb. J. Sci. 2019, 53, 1222–1228.

[35] Sultan, H.H.; Salem, N.; Al-Atabany, W. Multi-Classification of Brain Tumor Images Using Deep Neural Network. IEEE Access 2019, 7, 69215–69225.

[36] Kutlu, H.; Avcı; Avci, E. A Novel Method for Classifying Liver and Brain Tumors Using Convolutional Neural Networks, Discrete Wavelet Transform and Long Short-Term Memory Networks. Sensors 2019, 19, 1992.

[37] Swati, Z.N.K.; Zhao, Q.; Kabir, M.; Ali, F.; Ali, Z.; Ahmed, S.; Lu, J. Brain tumor classification for MR images using transfer learning and fine-tuning. Comput. Med. Imaging Graph. 2019, 75, 34–46.

[38] Shaikh, M.; Kollerathu, V.A.; Krishnamurthi, G. Recurrent Attention Mechanism Networks for Enhanced Classification of Biomedical Images. In Proceedings of the 2019 IEEE 16th International Symposium on Biomedical Imaging (ISBI 2019), Venice, Italy, 8–11 April 2019; pp. 1260–1264.

[39] Available Online: https://acsjournals.onlinelibrary.wiley.com/doi/full/10.3322/caac.21492.

[40] Rehman, A.; Naz, S.; Razzak, M.I.; Akram, F.; Razzak, I. A Deep Learning-Based Framework for Automatic Brain Tumors Classification Using Transfer Learning. Circuits Syst. Signal Process. 2019, 39, 757–775.

[41] Tripathi, P.C.; Bag, S. Non-invasively Grading of Brain Tumor Through Noise Robust Textural and Intensity Based Features. In Computational Intelligence in Pattern Recognition; Springer Science and Business Media LLC: Berlin/Heidelberg, Germany, 2019; pp. 531–539.

[42] Available Online: https://deepai.org/publication/deep-learning-based-brain-tumor-segmentation-a-survey.

[43] Kotia, J.; Kotwal, A.; Bharti, R. Risk Susceptibility of Brain Tumor Classification to Adversarial Attacks. In Proceedings of the Advances in Intelligent Systems and Computing, Krakow, Poland, 2–4 October 2019; pp. 181–187.

[44] Anaraki, A.K.; Ayati, M.; Kazemi, F. Magnetic resonance imaging-based brain tumor grades classification and grading via convolutional neural networks and genetic algorithms. Biocybern. Biomed. Eng. 2019, 39, 63–74.

[45] Abiwinanda, N.; Hanif, M.; Hesaputra, S.T.; Handayani, A.; Mengko, T.R. Brain Tumor Classification Using Convolutional Neural Network. In World Congress on Medical Physics and Biomedical Engineering 2018 Prague; Springer: Singapore, 2018; pp. 183–189.

[46] Kaldera, H.N.T.K.; Gunasekara, S.R.; Dissanayake, M.B. Brain tumor Classification and Segmentation using Faster R-CNN. In Proceedings of the 2019 Advances in Science and Engineering Technology International Conferences (ASET), Dubai, UAE, 26 March–10 April 2019; pp. 1–6.

[47] Kharrat, A.; Neji, M. Feature selection based on hybrid optimization for magnetic resonance imaging brain tumor classification and segmentation. Appl. Med. Inform. 2019, 41, 9–23.

[48] Available Online: https://www.sciencedirect.com/science/article/abs/pii/S1877750318307385.

[49] Amin, J.; Sharif, M.; Yasmin, M.; Fernandes, S.L. Big data analysis for brain tumor detection: Deep convolutional neural networks. Futur. Gener. Comput. Syst. 2018, 87, 290–297.

[50] 3D chemical imaging of brain tumors - Scientific Figure on ResearchGate. Available from: https://www.researchgate.net/figure/Brain-tumor-classification-based-on-tumor-location-29_fig1_333338321.

[51] Mohsen, Heba & El-Dahshan, El-Sayed & M.Salem, Abdel-Badeeh. (2012). A machine learning technique for MRI brain images. 2012 8th International Conference on Informatics and Systems, INFOS 2012. BIO-161.

[52] Zacharaki, Evangelia & Kanas, Vasileios & Davatzikos, Christos. (2011). Investigating machine learning techniques for MRI-based classification of brain neoplasms. International journal of computer assisted radiology and surgery. 6. 821-8. 10.1007/s11548-011-0559-3.